Challenge in Accurate Measurement of Fast Reversible Bimolecular Reaction

Kyril M. Solntsev[†] and Dan Huppert

School of Chemistry, Sackler Faculty of Exact Sciences, Tel-Aviv University, Tel Aviv 69978, Israel

Noam Agmon*

The Fritz Haber Research Center, Department of Physical Chemistry, The Hebrew University, Jerusalem 91904, Israel

Received: December 22, 2000; In Final Form: March 28, 2001

Reversible bimolecular chemical reactions of the AB ⇌ A + B type were predicted theoretically to deviate from exponential kinetics, obeying convolution kinetics at intermediate times and ultimately approaching equilibrium as a power law, $t^{-3/2}$, with a concentration-dependent amplitude. By careful application of time-resolved fluorescence methods, we verify these predictions for excited-state proton transfer from 2-naphthol-6,8-disulfonate to acidified water. The variation of the asymptotic amplitude with concentration is due predominantly to screening of the proton−anion Coulomb potential, and this masks the many-body effects on reversible binding itself. Better signal-to-noise in the long-time tails is required for clearly establishing the asymptotic behavior.

1. Introduction

Chemical reactions occur over a vast range of time scales.[1] Chemists routinely monitor reactions from femtoseconds (fs) to hours. Historically, only slow chemical reactions could have been monitored in the time domain, with samples regularly withdrawn to determine concentrations. The slowness of such monitoring processes could be overcome by spectroscopic methods. The tumble-stone then involved the requirement for fast initiation of the reaction. An important revolution in this respect came with the development of the relaxation techniques by Eigen and co-workers. For example, a temperature jump instantly modifies the reaction rate coefficients causing the chemical system to relax to a new equilibrium state. This enabled monitoring chemical reactions on the microsecond time scale. The method has been applied intensively to proton-transfer reactions.[2] Its results have led to the general understanding that for fast bimolecular chemical reactions in solution, diffusion cannot be separated from the chemical reaction step, and therefore the steady-state rate coefficients contain contributions from both processes.

The introduction of flash lamps, synchrotron radiation, and eventually short laser pulses again revolutionized chemical kinetics, enabling ultrafast initiation of ultrafast chemical reactions. Ground-state reactions may then be monitored by transient absorption, and excited-state reactions may be monitoried by time-resolved fluorescence.[3] One such monitoring technique involves time-correlated single-photon counting (TCSPC), recording first photon arrivals from the sample to the photomultiplier. Although limited in its picosecond time-resolution, it has extraordinary dynamic range and sensitivity, allowing the recording of signals over nearly five decades in intensity. With this kind of sensitivity, it becomes clear that it is not only the reaction rate coefficients that need be modified to include the effect of diffusion. The time evolution of concentrations of reactants or products of bimolecular reactions in solution can no longer be described by conventional exponential kinetics.

Our prototype AB ⇌ A + B reaction involves proton-transfer from the excited (fluorescing) singlet state (S_1) of a fluorophore.[4,5] In its excited-state (ES), the fluorophore becomes extremely acidic and consequently undergoes a process of proton-transfer to solvent (PTTS). At neutral pH with small photoacid concentrations (usually micromolars), homogeneously dissolved protons are on the average too far from the fluorophore to react with it during its ES lifetime. The fluorophore then undergoes reversible geminate recombination with the original proton.[6] Since these dissociation−recombination cycles are separated by diffusive motion, the role of diffusion in shaping the temporal behavior becomes pivotal, leading to an experimentally observed long-time power-law decay.[7−11]

At low pH, homogeneous protons compete with the geminate one for recombination, and the reaction becomes bimolecular. In fact, it is pseudo-unimolecular, because the concentration of the photoanion is much lower than that of the protons. Since the early work of Weller,[12] the pH effect on ES proton-transfer reactions has been described by biexponential kinetics.[13−19] A similar approach has been applied to other ES reactions, such as excimer formation.[20,21] Unfortunately, this treatment overlooks the most interesting many-body effects, which arise from competition over binding and occur between the initial dissociation event and final ES decay.

Modern approaches to reversible diffusion-influenced reactions have advanced considerably in recent years. A large body of theoretical work[22−35] and simulations[36−39] helped unravel the behavior of fast reversible reactions in solution. All agree that the approach to equilibrium can be markedly nonexponential. At short to intermediate times, it should be successfully represented by convolution kinetics, such as the convolution approximation (CA) approach.[25−27] At long times, this ap-

* To whom correspondence should be addressed.

[†] Also in the Department of Physical Chemistry, The Hebrew University, Jerusalem 91904, Israel. Present address: School of Chemistry and Biochemistry, Georgia Institute of Technology, Atlanta, GA 30332, USA.

10.1021/jp004569y CCC: $20.00
Published on Web 05/26/2001

proximation breaks down, and the kinetics switches into an asymptotic power-law behavior. The concentration dependence of its amplitude has recently been established.[30−34]

There were two previous attempts to detect these deviations from classical kinetics experimentally: in monomer−excimer kinetics[40] and ES-PTTS.[41] Signal-to-noise (S/N) problems (and poor graphical presentation of the results) hampered clear-cut conclusions. We have set out to obtain accurate kinetic data to check the theoretical predictions against experiment. The photoacid chosen for our study is 2-naphthol-6,8-disulfonate (2NDS) in acidified water. There has been ample work on this fluorophore.[42−46] Proton dissociation and rebinding occurs here considerably faster than ES decay. Consequently, the reaction attains equilibrium in its ES.[42] The high, pH-independent quantum yield[42,43] suggests that other kinetic complications, such as quenching by protons, are absent here.

The present work is unique in establishing the nonclassical approach to equilibrium in a reversible ES chemical reaction. By careful deconvolution of the data, we have managed to demonstrate the applicability of the CA, with subsequent switch-over to the predicted power-law regime. Unfortunately, the signal fades into the noise too early: To unravel the significant bimolecular effects on chemical reactivity, a new revolution in ultrafast kinetics is required, stressing accuracy rather than speed, improving the monitoring rather than the reaction initiation step.

2. The Theoretical Challenge

The kinetics of reversible chemical reactions, whether in the ground or excited states (ES), are traditionally described by conventional chemical kinetics.[1] Consider an excited hydroxyaryl (R*OH), dissociating in S_1 (rate coefficient k_d) to produce the excited conjugate base (R^*O^-). The latter, in turn, may associate bimolecularly with a proton (rate coefficient k_a) to regenerate the excited acid.

$$\begin{array}{ccc} R^*OH & \underset{k_a}{\overset{k_d}{\rightleftharpoons}} & R^*O^- + H^+ \\ \downarrow k_0 & & \downarrow k_0' \end{array}$$

When protons are in great excess, $c \equiv [H^+] \gg [R^*OH]$, and the pseudo-unimolecular recombination rate coefficient is ck_a. For equal ES lifetimes of acid and base ($1/k_0 = 1/k_0'$), the reaction is equivalent to AB $\rightleftharpoons$ A + B, when we set $[AB] = [R^*OH]\exp(k_0 t)$ and $[A] = [R^*O^-]\exp(k_0 t)$.

From simple chemical kinetics with no diffusional effects, the time-dependence of the relative concentration of the acid, given that initially ($t = 0$) only ROH has been excited, is given by

$$\frac{[R^*OH](t)}{[R^*OH](0)} = \frac{e^{-k_0 t}}{1 + cK_{eq}}\left[e^{-(k_d + ck_a)t} + cK_{eq}\right] \qquad (1)$$

Here K_{eq} is the ES equilibrium rate coefficient given by $K_{eq} = k_a/k_d$. The above solution starts from unity and decays to the ES equilibrium distribution, $cK_{eq}/(1 + cK_{eq})$, times the ES decay function, $\exp(-k_0 t)$. While the R*OH concentration decays biexponentially, the approach of $[R^*OH](t)\exp(k_0 t)$ to equilibrium is single exponential, $\exp[-(1 + cK_{eq})k_d t]$. This solution is at odds with the exact asymptotic solution for reversible diffusion-influenced reactions at long-times, and even with approximate solutions for the short/intermediate-time behavior, as described below.

2.1. Long-Time Asymptotics. When the relative diffusion of the dissociation products (diffusion coefficient $D = D_{RO^-} + D_{H^+}$) is taken into account, the conclusions from simple kinetic theory no longer hold. As three-dimensional diffusional effects develop, the kinetics slow and eventually switch into an asymptotic ($\sim$) power-law decay[30−34]

$$\frac{[R^*OH](t)}{[R^*OH](0)} \sim \frac{e^{-k_0 t}}{1 + cK_{eq}}\left[\frac{K_{eq}}{(1 + cK_{eq})^2 (4\pi D t)^{3/2}} + cK_{eq}\right] \qquad (2)$$

The equilibrium coefficient is given by

$$K_{eq} = k_a^{eff}/k_d \qquad (3)$$

where, in the absence of potential interactions (to be discussed below), $k_a^{eff} \equiv k_a$. It is convenient to denote

$$P(t) \equiv \frac{[R^*OH](t)}{[R^*OH](0)}\, e^{k_0 t} \qquad (4)$$

and $\Delta P(t;c) = P(t) - P(\infty)$. Its long-time approach to equilibrium

$$\Delta P(t; c) \sim \frac{K_{eq}}{(1 + cK_{eq})^3 (4\pi\, Dt)^{3/2}} \qquad (5)$$

depends only on K_{eq} and not on the individual rate parameters. As K_{eq} may be determined from the equilibrium plateau, $P(\infty) = cK_{eq}/(1 + cK_{eq})$, the asymptotic behavior could be tested *without* any adjustable parameters. Several theoreticians[22−34] have contributed to the development of this relation, which is now believed to be the exact asymptotic limit for the complicated, many-particle diffusion equation in which reversible reactivity was incorporated. Its geminate limit has been established both theoretically[8,25] and experimentally.[9] While power-laws have been discussed for irreversible diffusion influenced reactions,[47] their extension to reversible reactions is a more recent development. Possibly the first realization that the many-body approach to equilibrium is governed by power-law kinetics was made in the framework of fluctuation theory.[22,23] Equation 5 was derived from the asymptotics of the mean-field, nonlinear reaction−diffusion equations, except that printing errors obscured the result.[28] A truncated many-body theory, the "superposition-approximation" (SA),[24,26] gave a similar result but with a power 2 instead of 3 in the denominator. This disagreed with accurate one-dimensional simulations.[36,37] Subsequently, an enhanced SA[30,31] gave the correct power of $(1 + cK_{eq})$, and the agreement with the simulations motivated Szabo and co-workers to conjecture that eq 5 is the exact asymptotic solution.[30] This was recently proven mathematically using many-body recursion in Fourier space.[33,34] There was only one attempt to test eq 5 experimentally, for ES-PTTS, but the long time asymptotics was obscured by the noise.[41]

2.2. Short/Intermediate-Time Approximation. Classical chemical kinetics fails not only at asymptotically long times. If diffusion is not much faster than the rebinding reaction, dissociation enhances the local concentration of B-particles that surround A. The enhanced recombination regenerates the reactants and slows down the approach to equilibrium. This argument is made quantitative by the convolution approximation (CA) of Agmon and Szabo.[25−27] In the time interval between t' and $t' + dt'$ a fraction $k_d P(t')$ dissociates to the "contact distance", $r = a$. Denoting by $S_{irr}(t - t')$ the probability that this was the *last* dissociation event and thus A will not rebind during the remaining time, $t - t'$, one obtains

$$P(t) = 1 - k_d \int_0^t P(t')\, S_{irr}(t - t')\, dt' \qquad (6)$$

Given $S_{irr}(t)$, eq 6 can be solved iteratively starting with $P(0) = 1$. Since only final dissociation events are considered, S_{irr} is the "survival probability" for an irreversible boundary condition, $k_d = 0$. It corresponds to an "initial distribution" assumed to prevail immediately after a dissociation event, where all B-particles are randomly distributed except for one at $r = a$. By taking the product of the survival probabilities for the two kinds of B-particles one gets[25]

$$S_{irr}(t) = \frac{k_{irr}(t)}{k_a^{eff}} \exp[-c \int_0^t k_{irr}(t')\, dt'] \tag{7}$$

The preexponential on the right-hand side (rhs) is the survival probability due to the geminate B-particle at contact, whereas the second term is the celebrated Smoluchowski result for pseudo-unimolecular irreversible reactions.[47,48] The above relations become exact in the geminate limit (when $c = 0$), near $t = 0$ and at equilibrium.[25] Otherwise (for arbitrary times and concentrations), it is only an approximation, due to the assumption that the nongeminate particles are always randomly distributed.

The time-dependent irreversible rate coefficient, $k_{irr}(t)$, which corresponds to an initial random distribution for *all* particles, is given by the well-known expression[49,50]

$$k_{irr}(t) = \frac{k_D k_a^{eff}}{k_D + k_a^{eff}} \left[1 + \frac{k_a^{eff}}{k_D} \Psi(\gamma\sqrt{Dt})\right] \tag{8}$$

where $\Psi(z) = \exp(z^2)\mathrm{erfc}(z)$, erfc is the complementary error-function, k_D is the diffusion-control rate constant

$$k_D = 4\pi D a_{eff} \tag{9}$$

and the parameter γ is given by

$$\gamma a_{eff} = 1 + k_a^{eff}/k_D \tag{10}$$

In the absence of interactions, $k_a^{eff} = k_a$ and $a_{eff} = a$. The time integral in eq 7 may be performed analytically, but we make no use of this property here. Note that $k_{irr}(t)$ approaches $k_{irr}(\infty)$ as a power-law, because $\Psi(z) \sim 1/\sqrt{\pi}z$. This is not the power-law asymptotics of the reversible problem, although both arise from diffusion. The CA, in fact, does not show power-law asymptotics at all and is therefore valid only up to intermediate times.

The CA description was previously applied to pyrene excimer formation.[40] There, the initial state was that of an unbound excited monomer, surrounded by a uniform distribution of ground-state monomers. (This difference in initial conditions is not essential because a simple and rigorous relation exists between them.[25]) Reversibility became important at high temperatures, but, unfortunately, the data were displayed in a manner that makes it difficult to assess the merits of using the CA rather than the simpler kinetics of eq 1.

Equations 6 and 2 provide simple analytical descriptions for the approach to equilibrium in the short/intermediate and long time regimes, respectively. They require the knowledge of both rate parameters (not only their ratio), which we determine from a fit of the geminate kinetics ($c = 0$ limit) to the solution of a time-dependent Smoluchowski equation.[7−9] Unfortunately, the problem is further compounded by three effects that we have so far neglected. In the derivation of eq 2, it has been assumed that (i) A and AB are static, $D_A = D_{AB} = 0$; (ii) the ES lifetimes are equal, $k_0 = k_0'$; and (iii) there is no A−B interaction potential. The remainder of this section discusses the validity of these assumptions. Possibly, the first two are justified here, whereas the effect of the (screened Coulomb) potential between the proton and the conjugated base must be taken into account when implementing the CA.

2.3. Mobility Effects. The assumption of static A and AB molecules is not a bad approximation for PTTS reactions, since proton mobility exceeds that of large aromatic molecules by about an order of magnitude.[51] In practice, one usually takes $D = D_A + D_B$. One may scrutinize this approximation in light of recent results by Gopich, who has extended eq 2 to different (and nonvanishing) diffusivities.[52,53] This work shows that for mobile A and AB, eq 5 is still the exact long-time asymptotic solution, provided that

$$D = D_B + \frac{1}{1 + cK_{eq}}(D_A + cK_{eq}D_{AB}) \tag{11}$$

In our case, D_B (the proton diffusion coefficient) is dominant. The correction term, $(D_A + cK_{eq}D_{AB})/(1 + cK_{eq})$, contributes less than 10% and may thus be simplified. When $D_A \approx D_{AB}$ (a reasonable approximation for large aromatic acids and bases which differ only by one proton), this term reduces to D_A (or D_{AB}), and thus $D \approx D_A + D_B$ is indeed justified. We use for D_A the ground-state diffusion coefficient of the acid.

2.4. Different Lifetimes. The long-time behavior with which we wish to compare our experimental data, eq 5, has been derived for equal lifetimes. The only reversible diffusion problem that could be solved exactly for unequal lifetimes is the geminate limit.[54−58] A recent approximate theory for the many-body effect[35] suggests that at asymptotically long-times there should be a large observable effect of even a small difference in lifetimes. Let us assess the importance of taking this effect into account in the present case by considering the solution of the chemical kinetic equations for the different lifetime case[12−21]

$$\frac{[\mathrm{R^*OH}](t)}{[\mathrm{R^*OH}](0)} = \frac{1}{\lambda_1 - \lambda_2}[(\mu_1 - \lambda_2)e^{-\lambda_1 t} + (\lambda_1 - \mu_1)e^{-\lambda_2 t}] \tag{12}$$

The two exponents (eigenvalues) are given by

$$\lambda_{1,2} = [\mu_1 + \mu_2 \pm \Delta]/2 \tag{13}$$

where we have defined

$$\mu_1 \equiv k_d + k_0,\ \mu_2 \equiv ck_a + k_0' \tag{14a}$$

$$\Delta^2 \equiv (\mu_1 - \mu_2)^2 + 4ck_a k_d \tag{14b}$$

One may check that for $k_0 = k_0'$ eq 12 indeed reduces to eq 1.

To get a clearer picture of the changes occurring when $k_0 \neq k_0'$, let us make the further approximation that $|k_0 - k_0'|$ is small as compared to $k_d - ck_a$. This is a good approximation for ESPT from naphthol derivatives, whose ES lifetimes are typically in the range 5−15 ns, while they eject the proton on the subnanosecond time scale. Under such conditions $\Delta \approx k_d + ck_a$. The slowest exponent and its amplitude become

$$\lambda_2 \approx (k_0 + k_0')/2 \tag{15a}$$

$$\frac{\lambda_1 - \mu_1}{\lambda_1 - \lambda_2} \approx \frac{cK_{eq} - (k_0 - k_0')/(2k_d)}{1 + cK_{eq}} \tag{15b}$$

In our case $(k_0 - k_0')/(2k_d) \leq 0.001$, which could bias the

estimation of K_{eq} from the asymptotic plateau only at small concentrations. For the lowest concentration studied here (2.5 mM), the correction to K_{eq} amounts to at most 5%.

Next, consider the solution of the geminate problem for nonequal lifetimes.[54−57] It was verified experimentally that with decreasing $k_0 - k_0'$, the kinetics undergoes a (first-order) transition from power-law to exponential asymptotics.[58] The 2NDS anion is sufficiently long-lived for the power-law asymptotics to prevail. The asymptotic decay in this case is

$$\frac{[\mathrm{R^*OH}](t)}{[\mathrm{R^*OH}](0)} \sim \frac{Z^2 K_{eq} e^{-k_0' t}}{(4\pi D t)^{3/2}} \tag{16}$$

First, note that the exponential term is governed by k_0', rather than $(k_0 + k_0')/2$ as in eq 15a. Second, it is modified by the multiplicative factor $Z = k_{off}/(k_{off} + k_0 - k_0')$, where k_{off} is the overall separation rate coefficient. Thus, when dissociation is much faster than ES decay, which is the case considered here, $Z \approx 1$. On the basis of these arguments, we believe that the difference in lifetimes probably affects the equilibrium limit more than it affects the power-law approach to it.

2.5. Potentials. The final complication comes from the fact that we deal with ions,[51] rather than with noninteracting particles. Knowledge of their effective potential, $V(r)$, is important in implementing the CA, but not for the analysis of the long-time tail. In the latter case, we obtain $K_{eq}(c)$ from the asymptotic plateau (it is concentration-dependent due to the concentration-dependent effective potential) and use it in eq 5 to determine the asymptotic behavior.

The potential appears in the CA through the time-dependent rate-coefficient, $k_{irr}(t)$ of eq 8. We determine the interaction potential, $V(r)$ (in units of $k_B T$), by making two assumptions

$$k_a^{eff} = k_a e^{-V(a)} \tag{17a}$$

$$a_{eff} = \left(\int_a^\infty e^{V(r)} r^{-2} dr\right)^{-1} \tag{17b}$$

the first being more rigorous than the second. These two relations are substituted in eqs 7−10 instead of the simpler ones used in the absence of a potential (namely, $k_a^{eff} = k_a$ and $a_{eff} = a$). While the expression for the equilibrium coefficient, eq 3, remains exact, $k_{irr}(t)$ in eq 8 becomes an approximation, although usually a rather good one, which becomes exact at long times.[59]

We model the interaction potential by the Debye−Hückel screened Coulomb potential,[51]

$$V(r) = \frac{-R_D \exp[-\kappa_{DH}(r - a)]}{r(1 + \kappa_{DH} a)} \tag{18}$$

with an adjustable Debye−Hückel parameter, κ_{DH}. The "Debye radius" is calculated from $R_D = 560z/\epsilon$, where z is the charge of the counteranion and ϵ the solvent's dielectric constant. $1/\kappa_{DH}$ is the radius of the "ionic atmosphere". For univalent electrolytes, $\kappa_{DH} = Bc^{1/2}$ where $B = 0.33\ \mathrm{M}^{-1/2}$ in room temperature water. Since eq 18 cannot be rigorously true at short distances or high concentrations, we adjust B to fit the measured decrease in K_{eq} with increasing ionic strength. This, we shall see, is the dominant concentration effect on the asymptotic behavior for the reaction under investigation.

Ionic interactions also lead to a decrease in the diffusion coefficients of ions with increasing ionic strength.[51] We have detected this effect experimentally for geminate reactions when an inert salt was introduced.[60] Here the accuracy is insufficient to include this effect, so we use an estimated value of D for 10 mM salt.

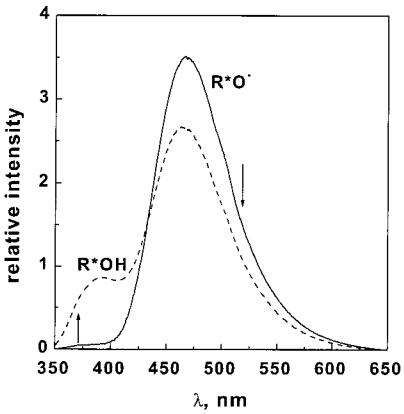

Figure 1. Emission spectra of 2NDS in water (solid line) and 50 mM HCl solution (dashed line). These solutions correspond to the two extreme proton concentrations used in this work, whereas the fluorophore concentration was kept constant. Position of vertical arrows indicate the wavelengths (370 nm for R*OH and 515 nm for R^*O^-) at which time-resolved measurements were performed. Direction of the arrows correspond to the increase of HCl concentrations.

3. Experimental Section

We have chosen to work on the photoacid 2-naphthol-6,8-disulfonate (2NDS) because it exhibits fast PTTS as compared to its ES lifetime(s) with little, if any, quenching by protons.[42−46] Since the sulfonate groups are on the distal ring, PTTS occurs directly to water and *not* through the sulfonate groups. Potassium salt of 2NDS was purchased from Kodak (>98% purity). Its absorbance did not exceed 0.2 at the excitation wavelength. All measurements were carried out at room temperature. Aqueous solutions with different hydrochloric acid concentrations were prepared volumetrically, by consequent dilution of standard 1.0075 N HCl solution (Aldrich, reagent grade) with 10 MΩ deionized water.

Steady-illumination fluorescence spectra of nondeoxygenated 2NDS solutions were recorded on a SLM-AMINCO-Bowman 2 luminescence spectrometer and corrected according to manufacturer specifications. The fluorescence spectrum consists of two structureless bands with R*OH emission maximum at 390 nm and R^*O^- maximum at 470 nm (Figure 1). With increasing acid concentration, c, the fluorescence intensity from R*OH increases while that of R^*O^- decreases. This clearly points to the reversibility of the reaction in the ES,[42] with equilibrium shifting to the acid form with increasing c.

To monitor PTTS in the time-domain, the sample was excited by a ps laser at about 300 nm (the doubled frequency of the Rhodamine 6G dye laser, driven by a Nd:YAG laser). Using a TCSPC system,[3] transient acid fluorescence was collected at 370 nm. We have also measured transient fluorescence from the base, by setting the monochromator to 515 nm. The full scale varied between 5 and 50 ns (corresponding to 4.88 and 48.8 ps/channel, respectively). Figure 2 shows an overview of the data at the two wavelengths as measured on the 50 ns time scale. As the acid intensity declines, the base signal rises. Eventually, both signals decay with the same rate coefficient (λ_2 in eq 12), indicating that the reaction has approached equilibrium.

The instrument response function (IRF) had a full-width at half-maximum of about 40 ps. We measure it using front-surface reflection from fused silica plates (the back-surface reflection

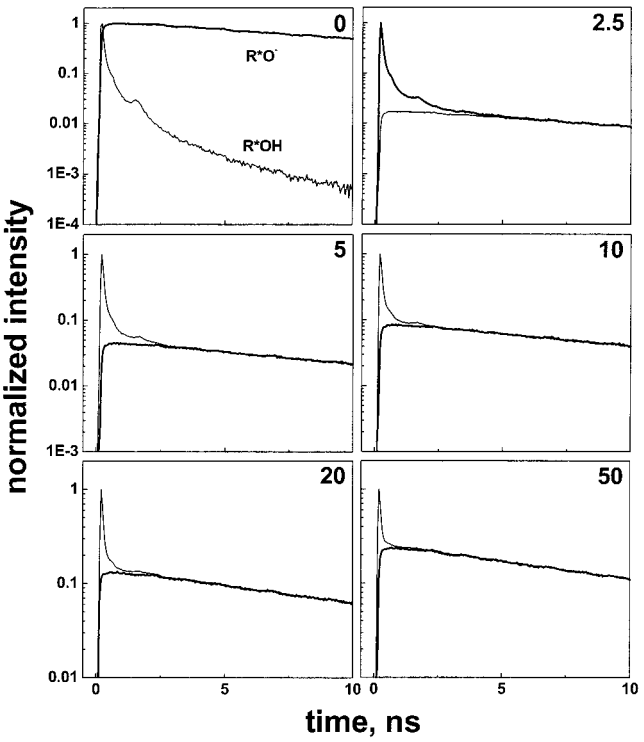

Figure 2. Normalized transient emission of 2NDS, measured on the 50 ns scale (first 10 ns shown) of the TCSPC apparatus at 370 nm (acid, light curves) and 515 nm (base, bold curves). The ultimate decay times at the different indicated proton concentrations (in mM), which (except for $c = 0$) are identical for both species, are τ_4 of Table 1. Note the semilog scale with the varying range for different panels.

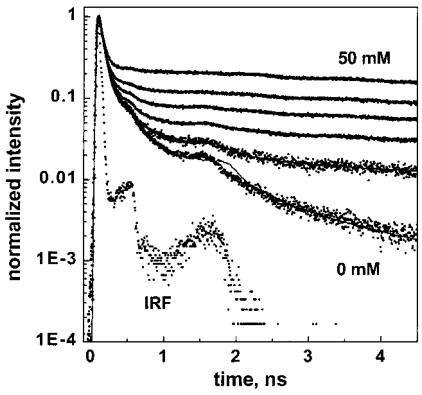

Figure 3. Unprocessed ROH emission data, collected at 370 nm on the 5 ns scale. Proton concentrations (top to bottom): 50, 20, 10, 5, 2.5, and 0 mM. Lowest data points are the laser flash (IRF). Lines are multiexponential fits to eq 19, convoluted with the IRF (except for $c = 0$, where it is a Smoluchowski fit using SSDP). The corresponding parameters are collected in Table 1.

is negligible). Figure 3 shows the raw R*OH data on the 5 ns scale, together with the IRF. It exhibits secondary parasitic peaks (less than 1% of main peak intensity) around 0.3 and 1.5 ns. These are seen to affect the measured signal for samples which decay fast to low count numbers (e.g., at low proton concentrations). Although we account for the IRF by convolution, the secondary peaks occur in physically significant time regions and tend to limit the accuracy of our measurement.

4. Data Analysis

The purpose of this work is to extract, from the measured fluorescence signals, the decay to equilibrium and compare it with the theoretical predictions in eqs 2 and 6. This is a demanding task in which one has to overcome (i) ES decay; (ii) low count numbers in the tails; (iii) aberrations due to secondary peaks in the IRF. We partially overcome these obstacles by the following deconvolution/smoothing procedure.

TABLE 1: Parameters[a] Obtained from Multi-Exponential Fits, Eq 19, on the 5 ns Scale of the TCSPC Apparatus

c, mM	τ_1, ns	τ_2, ns	τ_3, ns	τ_4, ns	A_1	A_2	A_3	A_4
0	0.0339	0.112	0.644	3.94	0.733	0.233	0.0294	0.0040
2.5	0.0405	0.131	0.770	12.15	0.772	0.197	0.022	0.0085
5	0.0393	0.125	0.687	12.00	0.766	0.195	0.0185	0.0206
10	0.0397	0.123	0.718	11.95	0.765	0.185	0.0127	0.0377
20	0.0347	0.109	0.821	11.90	0.742	0.193	0.0077	0.0577
50	0.0304	0.0885	1.92	11.50	0.685	0.210	0.0041	0.101

[a] Maximal standard errors for the τ_i: 2.6, 17, and 330 ps for $i = 1$, 2, 3, respectively. For $c > 0$, τ_4 was fixed at the values determined on the 50 ns scale. For $c = 0$, τ_4 does *not* reflect the ES decay time.

TABLE 2: Physical Parameters[a] Employed in Fitting the Geminate 2NDS Fluorescence Data Using Time-Resolved Smoluchowski Approach[7,8] via the SSDP Software[63]

D, cm^2/s	R_D, Å	a, Å	$1/k_d$, ps	k_a, M^{-1}s^{-1}	$1/k_0$, ns	$1/k_0'$, ns
9.5×10^{-5}	21.5	5.5	33	5.0×10^9	9.2	12.4

[a] D is sum of proton and anion diffusion coefficients[51]; R_D is the Debye radius for a triply charged ion in water[51]; the "contact radius", a, is a typical literature value[7,8]; k_0 is acid decay rate measured in acidic solutions pH ≈ -0.5; k_0' was estimated from anion decay in basic solutions (pH $\approx$ 12). Similar values were found in the literature: $1/k_0 = 8.4$ ns, $1/k_0' = 12.2$ ns[45] or $1/k_0 = 8.7$ ns, $1/k_0' = 12.8$ ns.[46] The value of k_d is similar to that in Figure 4 of ref 44.

First, we determine independently the lifetimes of the acid ($1/k_0$) and base ($1/k_0'$), by monitoring the fluorescence decay at low and high pH values, where only ROH or RO$^-$ exist in both ground and excited-states, and PTTS is suppressed. (We have, nevertheless, avoided using pH values much lower than 0, because of the proton quenching effect). The values obtained, see Table 2, are similar to literature values.[45,46]

Next, the longest time-constant [$\tau_4(c)$ in Table 1] is determined separately from the data series on the 50 ns scale (Figure 2). That $\tau_4(c) \approx 1/k_0'$ may be no accident: In the geminate case it was shown that k_0' should be used to "correct" the signal from *both* base and acid; see eq 16. This rule might extend to the pseudo-unimolecular case. In comparison, chemical kinetics suggests that $\tau_4 \approx 2/(k_0 + k_0')$, see eq 15a, which is not obeyed that well. Another observation is that τ_4 decreases slightly (up to 7%) with increasing proton concentration. This could reflect a small degree of quenching by protons that takes place for this molecule. It is negligible in comparison to some other naphthols[17,43] and was not detected previously in acid−base titrations.[42,43]

Further, the data on the 5 ns scale are fitted to a sum of four exponentials,

$$\frac{[\mathrm{R^*OH}](t)}{[\mathrm{R^*OH}](0)} = \sum_{i=1}^{4} A_i \exp(-t/\tau_i) \otimes \mathrm{IRF}(t) \qquad (19)$$

and convoluted with the IRF. It is normalized so that $\sum_{i=1}^{4} A_i = 1$. In these fits, τ_4 was held fixed, using the value obtained on the 50 ns scale. The lines in Figure 3 are the result of such fits, with the parameters (A_i, τ_i) collected in Table 1.

Multiexponential fits are commonly used as a deconvolution procedure in transient fluorescent measurements.[61,62] In our case, the multiexponential form is a natural choice, because the initial and final decay phases *are* exponential. The multiexponential fit serves several purposes in our analysis:

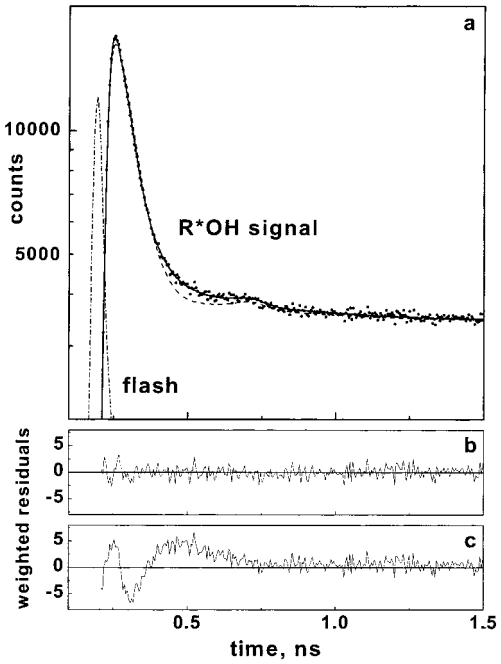

Figure 4. Comparison of the 2- and 4-exponential fits to the transient fluorescence of the 2NDS acid band in 50 mM HCl aqueous solution. Panel a compares the raw data (circles) with the 4-exponential fit (full line, residuals shown in panel b) and the 4-exponential fit (dashed line, residuals shown in panel c). It is clear that two exponentials are insufficient for fitting the data.

(i) It deconvolutes the bumpy IRF from our data, which otherwise masks the details of the approach to equilibrium.

(ii) It provides an objective determination of the asymptotic plateau, $cK_{eq}/(1 + cK_{eq})$, whose precise value affects the time-course for the deduced approach to equilibrium.

(iii) It smoothes the noisy data arising from the subtraction of this plateau.

The necessity of currently using such a procedure attests to the "challenge" in this kind of measurement.

One may wonder whether four exponentials are really necessary, since previous analyses of experimental data for this reaction[44−46] were content with the 2-exponential representation of eq 12. Figure 4 compares the 2- and 4-exponential fits for the highest concentration employed in this study (50 mM H^+). It is seen both from the fits and their residuals that 2-exponentials are insufficient to describe the fluorescence decay. The region between the initial and final exponential decays (around 0.5 ns) conceals the details of the approach to equilibrium.

τ_1 in eq 19 should be the proton dissociation time, and thus (within experimental error) independent of c. We can check this by comparison with the geminate kinetics. In the $c = 0$ limit, the pair kinetics obey the Smoluchowski equation, using D from mobility measurements and R_D from dielectric measurements.[7,8] The partial differential equation was solved numerically using the Windows application SSDP (ver. 2.6).[63] This produced the lowest line in Figure 3, with the physical parameters collected in Table 2. We see that indeed $k_d \approx 1/\tau_1$. Furthermore, the geminate rate parameters allow us to calculate the equilibrium constant at infinite dilution from eq 3, giving $K_{eq}(c = 0) = 8.8$ M^{-1}. The kinetics in water are fastest and thus most susceptible to complications from the secondary peaks in the IRF. This limits the accuracy in the determination of the rate parameters [hence also of $K_{eq}(0)$] to about 20%.

The automated multiexponential fitting procedure eliminates possible prejudice in determining the equilibrium plateau, which

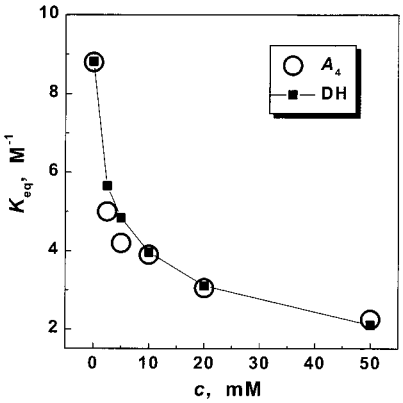

Figure 5. Ionic concentration dependence of the ES acid−base equilibrium coefficient for 2NDS. Circles are our experimental values from the multiexponential fit using eq 19. The infinite-dilution value was determined from the geminate parameters in Table 2. Squares represent the Debye−Hückel theory, eq 18, with adjusted $B = 0.46$ $M^{-1/2}$.

in the present approach is A_4 from eq 19. The equilibrium constant at low pH values may now be estimated, according to eqs 1 and 2, by

$$A_4 = cK_{eq}/(1 + cK_{eq}) \tag{20}$$

These K_{eq} values are shown by the open circles in Figure 5. They are compared with the Debye−Hückel (DH) prediction, eq 18 (squares). To achieve the fit, we use the same radius, a, as in the diffusive dynamics, but adjust the DH parameter to $B = 0.46$ $M^{-1/2}$ (instead of its theoretical value of 0.33). Agreement is good, except at the lowest concentrations (2.5 and 5 mM), where A_4 gives values that are too small by about 20%. One source for this discrepancy is the nonequality of the two ES lifetimes, which could lead to correction terms such as in eq 15b. Since $k_0 - k_0' > 0$, this should increase K_{eq} (by about 0.5 M^{-1}, see parameters in Table 2).

The approach to equilibrium at different concentrations, $\Delta P(t; c)$, can now be calculated from

$$\Delta P(t; c) \equiv \sum_{i=1}^{3} A_i \exp(-t/\tau_i + t/\tau_4) \tag{21}$$

It is depicted by the bold lines in Figures 6 and 7, which represent our smoothed and deconvoluted data. The initial decay is due to dissociation alone, $\exp(-k_d t)$, as depicted by the dash−dot curve in Figure 6. This is identical with the prediction of kinetic theory, namely, $\exp[-k_d(1 + cK_{eq})t]$, because $cK_{eq} \ll 1$ (it is at most 0.1 at $c = 50$ mM). Clearly, therefore, the exponential kinetics of eq 1 is inappropriate for describing our data.

In contrast, the CA yields very good results for over 2 orders of magnitude (dashed lines, Figure 6). These results were obtained by solving, using numerical iterations, the convolution relation 6. The parameters that go into this theory (eqs 6−10, 17, and 18) are available from independent measurements (Table 2). The diffusion coefficients are from mobility measurements,[51] R_D is evaluated for the triply charged anion from the water dielectric constant ($\epsilon = 78$), k_d and k_a were obtained by fitting the geminate data to the transient Smoluchowski equation using SSDP (ver. 2.6),[63] and B was obtained by fitting the Debye−Hückel potential, eq 18, to $K_{eq}(c)$ in Figure 5. In practice, we have fine-tuned some of the parameters within their error-bars to obtain consistency. We believe Figure 6 provides a convincing demonstration for the applicability of the CA.

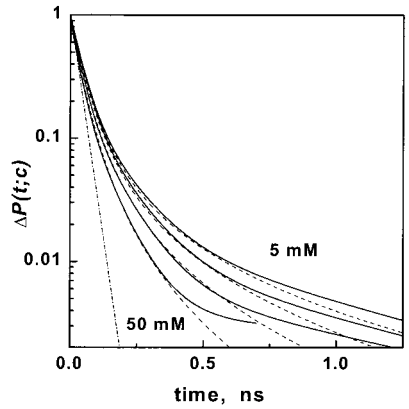

Figure 6. Approach to equilibrium in a reversible ES pseudo-first PTTS reaction. Fluorescence data from excited 2NDS in aqueous acidic solutions of various proton concentrations (top to bottom: 5, 10, 20, and 50 mM HCl) were processed by the multiexponential deconvolution approach (eq 21, full curves). Dashed lines show the prediction of convolution kinetics,[25] eqs 6−10, 17, and 18, with independently determined parameters. For comparison, a dash−dot line depicting exponential decay, $\exp(-k_d t)$, is also shown.

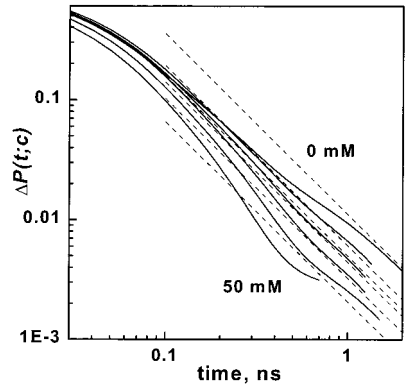

Figure 7. Approach to equilibrium in a reversible ES pseudo-first PTTS reaction. Same data as in Figure 6, for proton concentrations (top to bottom) 0, 2.5, 5, 10, 20, and 50 mM, in a log−log scale (full curves). The theoretical asymptotic behavior from eq 22, using experimental K_{eq} values from Figure 5, is shown by the dashed lines.

At asymptotically long times the CA ceases to apply, and the kinetics switch over to power-law decay: A straight line on the log−log plot. Figure 7 shows our deconvoluted data (eq 21) on this scale. Since the signal fades in the noise after the third exponential, these curves are truncated at about $2\tau_3$. The dashed lines are the theoretical asymptotic behavior, eq 5. It may be written as

$$\Delta P(t; c) \sim \frac{K_{eq}(c)}{K_{eq}(0)} \frac{\Delta P(t; 0)}{[1 + cK_{eq}(c)]^3} \qquad (22)$$

In the geminate limit,[8] $\Delta P(t; 0) \sim K_{eq}(0)(4\pi Dt)^{-3/2}$ can again be calculated from the SSDP parameters [$K_{eq}(0) = 8.8$ M^{-1} and $D = 9.5 \times 10^{-5}$ cm^2/s]. The asymptotic behavior at higher concentrations then requires only $K_{eq}(c)$, which were already determined from the equilibrium plateau, A_4 (see Figure 5).

The novelty and limitations of these results should be acknowledged. The figure provides a first clear demonstration that $\Delta P(t; c)$ indeed switches into a $t^{-3/2}$ asymptotic behavior. Theory appears to describe the asymptotic behavior well, and with no adjustable parameters. Interestingly for the present system, the many-body competition term, $1/(1 + cK_{eq})^3$, makes a negligible contribution. The main contribution to the variation of $\Delta P(t; c)/\Delta P(t; 0)$ comes from the concentration dependence of the equilibrium coefficient, which originates from many-body effects on the *interaction potential*. We acknowledge that the data leave more to be desired, as it fades into the noise just as it reaches the asymptotic line, whereas one would like to see the $t^{-3/2}$ law followed for longer times.

Finally, a closer inspection of the data in Figure 7 suggests a *second-order* transition in the kinetics. The asymptotic behavior is always $t^{-3/2}$, but the approach to it changes with concentration. At low concentrations, $\Delta P(t; c)$ begins below the asymptotic line, then crosses it and converges in from above. At high concentrations, the situation is reversed: $\Delta P(t; c)$ begins above the asymptotic line, crosses it and converges in from below. Such detail are outside the scope of the CA. However, an analogous transition has been found in geminate recombination with two different lifetimes,[57] where a "second-order" transition was manifested in approach to the asymptotic line from above or below. Clearly, more accurate data are needed to establish this interesting effect.

5. Discussion

The present work considered excited-state reactivity of photoacids, yet it has direct consequences to a much broader family of chemical reactions, namely, bimolecular binding reactions of the AB ⇌ A + B type. Such reactions include fundamentally important processes such as acid−base reactions, hormone and transmitter binding to receptors, substrate binding to an active site, and more. When these reactions are intrinsically fast and reversible, many-body diffusion effects are expected to lead to marked deviations from classical kinetics. These effects have been considered theoretically yet overlooked by photochemists who have studied photoacids extensively, predominantly by transient fluorescence techniques. The present study provides one of the first convincing experimental examples for the predicted effects.

We work with photoacids because excitation provides an ultrafast means to initiate their dissociation reaction. Otherwise, there is no fundamental difference between excited-state and ground state reactivity, particularly so when reactants and products share the same excited-state lifetime. The excited photoacid corresponds to a special initial condition of an AB molecule surrounded by equilibrated B molecules. Often, one is interested in another initial condition, of an unbound A molecule surrounded by B's. Since a simple and rigorous relation exists between the solutions for these two initial conditions,[25] the understanding of one immediately implies understanding of the other. The present work extends our previous work of geminate recombination to the pseudo-unimolecular case (one A, many B's), where the concentration (of B particles) becomes an important variable. Understanding of the unimolecular case paves the road to further extension to arbitrary A and B concentrations.[53]

Our work is unique in unraveling some of the details in the nonexponential approach to equilibrium of excited 2-naphthol-6,8-disulfonate. Deconvoluting/smoothing the fluorescence data using a 4-exponential fit and subtracting the equilibrium plateau reveals how poorly classical kinetics describes this simple solution-phase reaction. As Figure 6 showed, the nonexponential effects are substantial, starting around 50 ps for this reaction, and dominating most of the transient behavior. Thus, more sophisticated kinetic theories must be applied. We find that the short/intermediate time behavior agrees with the Agmon-Szabo convolution kinetics[25] for over two decades in intensity. To our knowledge, this is the first time such an agreement is demon-

strated. Moreover, all the parameters required for this model can, in principle, be gleaned from independent measurements. In this theory, the geminate partner which has just dissociated to the contact distance contributes to the recombination probability on top of the population of uniformly distributed protons.

Close to equilibrium, however, the assumption of a uniform distribution for the homogeneous protons breaks down and so does convolution kinetics. The approach to equilibrium now switches into the theoretically predicted $t^{-3/2}$ decay. Moreover, the theoretical amplitude of this power-law phase, $K_{eq}/(1 + cK_{eq})^3$, agrees with experiment with no adjustable parameters (given K_{eq} obtained from the equilibrium plateau). This provides rather compelling evidence for the role of diffusion in determining the transient evolution of bimolecular, reversible chemical reactions.

The theoretical amplitude contains two contributions. K_{eq} in the numerator prevails also in the geminate ($c = 0$) limit. It arises from diffusing pairs reaching their contact distance, at which they are in quasi-equilibrium with the bound state. The many-body effect on the asymptotic behavior is manifested in the $(1 + cK_{eq})^{-3}$ term,[30,31] which arises from single re-encounters of the excited base with a given proton which are possibly separated in time by single encounters with other protons.[33,34] Unfortunately for the reaction under investigation, as we lower the pH, the variation in this term is about an order of magnitude less than the variation in K_{eq}. The latter decreases sharply due to increasing ionic screening, in qualitative agreement with the Debye−Hückel (DH) theory for activity coefficients. Hence, we are not able to demonstrate experimentally the many-body competition effect, manifested in the $(1 + cK_{eq})^{-3}$ term, nor show that the power is indeed 3 (and not 2, as suggested by earlier theoretical approaches[26]). To fit the concentration dependence of K_{eq}, the ionic atmosphere radius in the DH theory was modified. Given the present experimental accuracy and the uncertainty in the molecular radius, a, this does not necessarily indicate a break-down of this celebrated theory. Finally, we observe an interesting kinetic transition, where at a critical concentration the approach to equilibrium changes from below to above the asymptotic line.

Clearly, enhanced experimental sensitivity and accuracy are desired. Hopefully, the IRF of the TCSPC apparatus could be improved to eliminate, as much as possible, the spurious low-amplitude peaks that get convoluted with the kinetics at critical time epochs. Other efforts should be directed into improving the S/N in the tails. The TCSPC apparatus registers events of first photon arrivals, most of which occur near the peak of the R*OH signal, during the initial exponential dissociation phase. If one could block the photons from this initial phase (e.g., for the first 100 ps in our case), all the photon-arrival statistics would concentrate in the nonexponential tail. This calls for the design of an appropriate electronic gating apparatus.

We believe our results demonstrate that there is significant information concealed in the transient behavior of fast bimolecular reactions. To unravel this information, a new revolution in fluorescence kinetics is required, with emphasis on accuracy and low noise levels of the measured signals.

Acknowledgment. Work supported in part by grants from the Israel Science Foundation, administered by the Israel Academy of Sciences and by the James-Franck German-Israel program in laser-matter interaction. The Fritz Haber Research Center is supported by the Minerva Gesellschaft für die Forschung, mbH, München, FRG.

References and Notes

(1) Laidler, K. J. *Chemical Kinetics*; Harper and Row: New York, 3rd ed., 1987.
(2) Eigen, M.; Kruse, W.; Maass, G.; De Maeyer, L. *Prog. React. Kinet.* **1964**, *2*, 287−318.
(3) Lakowicz, J. R. *Topics in Fluorescence Spectroscopy*; Plenum Press: New York, 1991.
(4) Förster, T. *Z. Elektrochem.* **1950**, *54*, 42−46.
(5) Weller, A. *Prog. React. Kinet.* **1961**, *1*, 187−214.
(6) Pines, E.; Huppert, D. *J. Chem. Phys.* **1986**, *84*, 3576−3577.
(7) Pines, E.; Huppert, D.; Agmon, N. *J. Chem. Phys.* **1988**, *88*, 5620−5630.
(8) Agmon, N.; Pines, E.; Huppert, D. *J. Chem. Phys.* **1988**, *88*, 5631−5638.
(9) Huppert, D.; Pines, E.; Agmon, N. *J. Opt. Soc. Am. B* **1990**, *7*, 1545−1550.
(10) Agmon, N.; Huppert, D.; Masad, A.; Pines, E. *J. Phys. Chem.* **1991**, *95*, 10407−10413. Erratum: *J. Phys. Chem.* **1992**, *96*, 2020.
(11) Solntsev, K. M.; Agmon, N. *Chem. Phys. Lett.* **2000**, *320*, 262−268.
(12) Weller, A. *Z. Phys. Chem. NF* **1958**, *15*, 438−453.
(13) Loken, M. R.; Hayes, J. W.; Gohlke, J. R.; Brand, L. *Biochem.* **1972**, *11*, 4779−4786.
(14) Ireland, J. F.; Wyatt, P. A. H. *Adv. Phys. Org. Chem.* **1976**, *12*, 131−221.
(15) Laws, W. R.; Brand, L. *J. Phys. Chem.* **1979**, *83*, 795−802.
(16) Harris, C. M.; Selinger, B. K. *J. Phys. Chem.* **1980**, *84*, 891−898.
(17) Webb, S. P.; Philips, L. A.; Yeh, S. W.; Tolbert, L. M.; Clark, J. H. *J. Phys. Chem.* **1986**, *90*, 5154−5164.
(18) Krishnan, R.; Fillingim, T. G.; Lee, J.; Robinson, G. W. *J. Am. Chem. Soc.* **1990**, *112*, 1353−1357.
(19) Lima, J. C.; Abreu, I.; Brouillard, R.; Maçanita, A. L. *Chem. Phys. Lett.* **1998**, *298*, 189−195.
(20) Birks, J. B. *Photophysics of Aromatic Molecules;* Wiley-Interscience: London, 1970.
(21) Kuz'min, M. G.; Sadovskii, N. A. *High Energy Chem.* **1975**, *9*, 255−270.
(22) Zel'dovich, Ya. B.; Ovchinnikov, A. A. *Sov. Phys. JETP* **1978**, *47*, 829−837.
(23) Kang, K.; Redner, S. *Phys. Rev. A* **1985**, *32*, 435−447.
(24) Lee, S.; Karplus, M. *J. Chem. Phys.* **1987**, *86*, 1883−1903.
(25) Agmon, N.; Szabo, A. *J. Chem. Phys.* **1990**, *92*, 5270−5284.
(26) Szabo, A. *J. Chem. Phys.* **1991**, *95*, 2481−2490.
(27) Berberan-Santos, M. N.; Martinho, J. M. G. *J. Chem. Phys.* **1991**, *95*, 1817−1824.
(28) Burlatsky, S. F.; Oshanin, G. S.; Ovchinnikov, A. A. *Chem. Phys.* **1991**, *152*, 13−21.
(29) Gopich, I. V.; Doktorov, A. B. *J. Chem. Phys.* **1996**, *105*, 2320−2332.
(30) Naumann, W.; Shokhirev, N. V.; Szabo, A. *Phys. Rev. Lett.* **1997**, *79*, 3074−3077.
(31) Sung, J.; Shin, K. J.; Lee, S. *J. Chem. Phys.* **1997**, *107*, 9418−9436.
(32) Sung, J.; Lee, S. *J. Chem. Phys.* **1999**, *111*, 10159−10170.
(33) Gopich, I. V.; Agmon, N. *Phys. Rev. Lett.* **2000**, *84*, 2730−2733.
(34) Agmon, N.; Gopich, I. V. *J. Chem. Phys.* **2000**, *112*, 2863−2869.
(35) Kwac, K.; Yang, M.; Shin, K. J. *J. Chem. Phys.* **2001**, *114*, 3883−3897.
(36) Agmon, N.; Edelstein, A. L. *J. Chem. Phys.* **1994**, *100*, 4181−4187.
(37) Edelstein, A. L.; Agmon, N. *J. Phys. Chem.* **1995**, *99*, 5389−5401.
(38) Kim, H.; Yang, M.; Shin, K. J. *J. Chem. Phys.* **1999**, *111*, 1068−1075.
(39) Popov, A. V.; Agmon, N. *Chem. Phys. Lett.* **2001**, in press.
(40) Martinho, J. M. G.; Farinha, J. P.; Berberan-Santos, M. N.; Duhamel, J.; Winnik, M. A. *J. Chem. Phys.* **1992**, *96*, 8143−8149.
(41) Huppert, D.; Goldberg, S. Y.; Masad, A.; Agmon, N. *Phys. Rev. Lett.* **1992**, *68*, 3932−3935.
(42) Schulman, S. G.; Rosenberg, L. S.; Vincent, W. R., Jr. *J. Am. Chem. Soc.* **1979**, *101*, 139−142.
(43) Zaitsev, N. K.; Demyashkevich, A. B.; Kuz'min, M. G. *High Energy Chem.* **1979**, *13*, 288−293.
(44) Huppert, D.; Kolodney, E.; Gutman, M.; Nachliel, E. *J. Am. Chem. Soc.* **1982**, *104*, 6949−6953.
(45) Bardez, E.; Monnier, E.; Valeur, B. *J. Phys. Chem.* **1985**, *89*, 5031−5036.
(46) Das, R.; Mitra, S.; Nath, D.; Mukherjee, S. *J. Phys. Chem.* **1996**, *100*, 14514−14519.
(47) Rice, S. A. *Diffusion-Limited Reactions*; *Comprehensive Chem. Kinet.* Elsevier: Amsterdam, 1985; Vol 25.
(48) von Smoluchowski, M. *Z. Physik. Chem.* **1917**, *92*, 129−168.

(49) Collins, F. C.; Kimball, G. E. *J. Colloid Sci.* **1949**, *4*, 425−437.
(50) Gösele, U. M. *Prog. React. Kinet.* **1984**, *13*, 63−161.
(51) Robinson, R. A.; Stokes, R. H. *Electrolyte Solutions*, 2nd ed.; Butterworth: London, 1959.
(52) Gopich, I. V., **1999**, unpublished.
(53) Gopich, I. V.; Ovchinnikov, A. A.; Szabo, A. *Phys. Rev. Lett.* **2001**, *86*, 922−925.
(54) Agmon, N.; Gopich, I. V. *Chem. Phys. Lett.* **1999**, *302*, 399−404.
(55) Gopich, I. V.; Solntsev, K. M.; Agmon, N. *J. Chem. Phys.* **1999**, *110*, 2164−2174.
(56) Agmon, N. *J. Chem. Phys.* **1999**, *110*, 2175−2180.
(57) Gopich, I. V.; Agmon, N. *J. Chem. Phys.* **1999**, *110*, 10433−10444.
(58) Solntsev, K. M.; Huppert, D.; Agmon, N. *Phys. Rev. Lett.* **2001**, *86*, 3427−3430.
(59) Szabo, A. *J. Phys. Chem.* **1989**, *93*, 6929−6939.
(60) Agmon, N.; Goldberg, S. Y.; Huppert, D. *J. Mol. Liquids* **1995**, *64*, 161−195.
(61) Maroncelli, M.; Fleming, G. R. *J. Chem. Phys.* **1987**, *86*, 6221−6239.
(62) O'Connor, D. V.; Phillips, D. *Time-Correlated Single Photon Counting;* Academic Press: London, 1984; Chapter 6.
(63) Krissinel', E. B.; Agmon, N. *J. Comput. Chem.* **1996**, *17*, 1085−1098.